Spacecraft Attitude Control Using Approximate Receding-Horizon Model-Error Control Synthesis

Jongrae Kim*

University of Leicester, Leicester LE1 7RH, UK

John L. Crassidis†

University at Buffalo, State University of New York, Amherst, NY 14260-4400

Model-error control synthesis is a nonlinear robust control approach that mitigates the effects of modeling errors and disturbances on a system by providing corrections to the nominal control input directly. In this paper model-error control synthesis is applied to the spacecraft attitude control problem, where the model-error vector is computed using a receding-horizon approximation. The main advantage of this approach over other adaptive approaches for spacecraft attitude control is that it can simultaneously handle both inertia modeling errors and time varying disturbances. A design scheme is presented to determine the weighting factor and the length of the associated receding-horizon interval of the model-error solution by minimizing the closed-loop sensitivity norm. Simulation results are provided to show the performance of the new control approach.

I. Introduction

Model-error control synthesis (MECS) is a signal synthesis adaptive control method.[1] Robustness is achieved by applying a correction control to the nominal control vector, thereby minimizing the effects of modeling errors and disturbances at the system output.[2,3] The model-error vector is determined by using either a one-step ahead prediction approach[1,4] or an Approximate Receding-Horizon (ARH) approach.[5] As shown by the benchmark problem example in Ref. 4, the one-step ahead prediction approach inherent in MECS could not stabilize the system for the given ranges of uncertainties, which has one pole at the origin and two poles on the imaginary axis. When using the ARH approach the closed-loop system can tolerate relatively larger uncertainties than the one-step ahead prediction approach. However, the one-step ahead prediction approach may be easier to design for complicated systems than the ARH approach. Therefore, choosing between the one-step ahead prediction approach or the ARH approach to determine the model error depends on the particular properties and required robustness in the system to be controlled.

In Ref. 1 MECS with the one-step ahead prediction approach is first applied to suppress the wing rock motion of a slender delta wing, which is described by a highly nonlinear differential equation. Results indicated that this approach provides adequate robustness for this particular system. In Ref. 4 a simple study to test the stability of the closed-loop system is presented using a Padé approximation for the time delay inherent in the MECS approach, which showed the relation between the system zeros and the weighting in the cost function. The analysis proved that some systems cannot be stabilized using the original model-error estimation algorithm, which lead to the ARH approach in the MECS design to determine the model-error vector in the system.[5] A closed-form solution of the ARH approach using Quadratic Programming (QP) is first presented by Lu.[6] Although the problem is solved from a control standpoint, the algorithm must be reformulated as an estimation problem to determine the model-error vector, which is discussed in this current paper.

The control of spacecraft for large-angle slewing maneuvers poses a difficult problem, which is mainly due to the highly nonlinear characteristics of the governing equations. Much effort has been devoted to the

*Research Associate, Department of Engineering. Email: jrk7@le.ac.uk. Member AIAA.

†Associate Professor, Department of Mechanical & Aerospace Engineering. Email: johnc@eng.buffalo.edu. Associate Fellow AIAA.

closed-loop design of spacecraft with large angle slews. In fact, many viable and practical stable control laws have reached mainstream use today on several missions, including the International Space Station.[7] Current research focuses on the development of adaptive control laws that maintain desired closed-loop dynamics in the presence of modeling errors and disturbances. Ahmed et al.[8] present an approach that identifies the inertia matrix in real time and proves that the process is asymptotically stable. Schaub et al.[9] expand upon this approach by also estimating for disturbance inputs. The disadvantages of these adaptive approaches are the state vector must be appended to estimate the parameters and the parameters themselves, including the disturbance inputs, must be constant. A disturbance accommodating technique has been developed to handle time varying disturbances,[10] but this approach requires the use of specific basis functions to characterize the disturbance. Still, these approaches form a foundation to provide robustness for large-angle spacecraft slewing maneuvers.

In this paper the MECS approach with the ARH solution is applied to the spacecraft attitude control problem, which is an expansion of the approach presented in Ref. 13. The advantages of this approach over the aforementioned approaches for large-angle spacecraft slewing maneuvers include: 1) the MECS approach does not require appending the state vector to estimate for the unknown parameters, and 2) it can handle time varying disturbances without assuming any form for these disturbances. In Ref. 9 an adaptive control approach using attitude, based on the Modified Rodrigues Parameters (MRP), and angular-velocity information has been developed. This approach provides robustness in the system by estimating the inertia matrix and (assumed constant) external disturbances through a linear closed-loop dynamics expression. The development of the MECS approach in our work retains the same basic non-adaptive portion of the controller in Ref. 9 for the nominal controller, however, instead of estimating each element of the inertia matrix and the external disturbance separately, the whole effect of both uncertainties is estimated by the ARH approach through a model-error vector in the dynamics. The MECS approach subtracts the determined model error from the nominal control input in order to track the desired dynamics in the face of bounded inertia and external disturbance errors. This paper expands upon the results of Ref. 13 to include a stability analysis of of the overall system with modeling errors included.

The organization of this paper is as follows. First, the ARH approach to determine the model-error vector in a system is summarized. As an alternative form to the original ARH solution the state prediction in the ARH approach is modified using a higher-order Taylor series expansion. Second, the new approach is applied to the spacecraft attitude control problem. A design scheme is presented to determine the weighting factor and the length of receding-horizon interval to minimize the sensitivity function norm of the closed-loop system. Next, a nonlinear analysis of the spacecraft attitude control system using MECS is shown. Finally, results for spacecraft attitude maneuvers are shown through simulation.

II. Approximate Receding-Horizon Solution

In this section the basic concept of MECS is introduced, where the model error is determined as a solution of the approximate receding-horizon optimization problem.

A. MECS Concept

The overall MECS system block diagram is shown in Figure 1, where $\mathbf{x}(t)$ is the state vector and $\mathbf{r}(t)$ is the reference vector. The model error is determined using the system states, the control input and the current measurement. The determined model error, $\hat{\mathbf{u}}(t)$, corrects the nominal control input, $\bar{\mathbf{u}}(\mathrm{t})$, to provide an overall control input, $\mathbf{u}(t)$. Since a response in the system must be given before compensation is applied, the following model error correction input is used:[1]

$$\mathbf{u}(t) = \bar{\mathbf{u}}(t) - \hat{\mathbf{u}}(t-\tau) \tag{1}$$

where $\bar{\mathbf{u}}(t)$ is the nominal control input at time t, which can be any controller, and $\hat{\mathbf{u}}\,(t-\tau)$ is the estimated model error at time $t-\tau$, determined by the solution of the ARH problem. The time delay τ is always present in the overall MECS design because the measurement of the output $\mathbf{y}(t)$, denoted by $\tilde{\mathbf{y}}(t)$, must be given before the error in the system can be corrected. For discrete-time measurement systems the time delay can be set to the sampling interval. If the time delay is much longer than the expected, the error correction may yield some adverse effects in the response and, in the worst case, the closed-loop system may unstable. However, our experience has indicated that for most systems whose sampling rate is below Nyquist's upper

limit, this time delay causes no significant problems on stability. Still, the robustness with respect to some range of time delay on the performance response has to be checked during the design procedure.

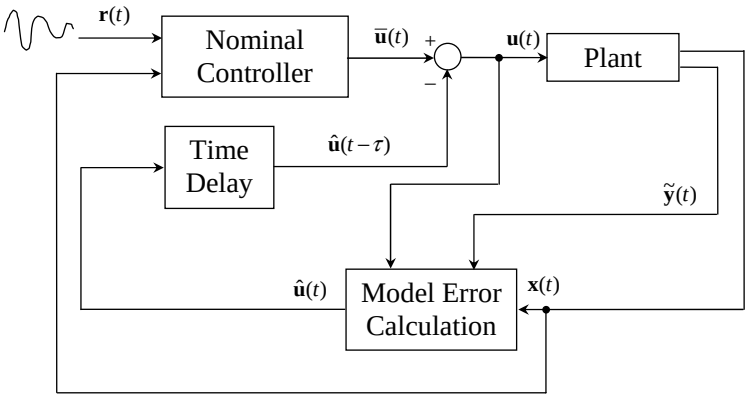

Figure 1. MECS Block Diagram

B. Model Error Determination

To determine the model error in a system, the receding-horizon optimization problem is set up as follows:[6]

$$\min_{\hat{\mathbf{u}}} J\left[\mathbf{x}(t),\, t,\, \hat{\mathbf{u}}(t)\right] = \int_t^{t+T} \left[\mathbf{e}^T(\xi)\, R^{-1}(\xi)\, \mathbf{e}(\xi) + \hat{\mathbf{u}}^T(\xi)\, W(\xi)\, \hat{\mathbf{u}}(\xi)\right] d\xi \tag{2}$$

subject to

$$\dot{\mathbf{x}}(t) = \mathbf{f}\left[\mathbf{x}(t)\right] + G\left[\mathbf{x}(t)\right]\mathbf{u}(t) + G\left[\mathbf{x}(t)\right]\hat{\mathbf{u}}(t) \tag{3a}$$

$$\mathbf{y}(t) = \mathbf{c}\left[\mathbf{x}(t)\right] \tag{3b}$$

with the initial condition, $\mathbf{x}_0 = \mathbf{x}(0)$, where R and W are positive definite and positive semi-definite weighting matrices, respectively, $\mathbf{f}\left[\mathbf{x}(t)\right] : \Re^n \to \Re^n$ is the assumed model vector, $G\left[\mathbf{x}(t)\right] : \Re^n \to \Re^{n\times q}$ is assumed control-input and model-error distribution matrix, $\mathbf{x}(t) \in \Re^n$ is the state vector, $\mathbf{u}(t) \in \Re^q$ is the control input, $\hat{\mathbf{u}}(t) \in \Re^q$ is the to-be-determined model error, $\mathbf{c}\left[\mathbf{x}(t)\right] : \Re^n \to \Re^m$, and $\mathbf{y}(t) \in \Re^m$ is the assumed system output. Both $\mathbf{f}\left[\mathbf{x}(t)\right]$ and $G\left[\mathbf{x}(t)\right]$ are C^2, where the first and the second derivatives are continuous and $\mathbf{c}\left[\mathbf{x}(t)\right]$ is sufficiently differentiable. In addition, $\mathbf{f}\left(\mathbf{0}\right)$ is equal to zero (if not, we can transform the states $\mathbf{x}(t)$ to some new states so that this condition holds). Also, we assume that a unique solution for $\mathbf{x}(t)$ exists. In the receding-horizon problem the error at the end of horizon is forced to be equal to zero as follows:

$$\mathbf{e}(t+T) = 0 \tag{4}$$

where the residual error is defined by

$$\mathbf{e}(t) = \tilde{\mathbf{y}}(t) - \mathbf{y}(t) \tag{5}$$

where the measurement of the output, $\tilde{\mathbf{y}}(t)$, may include zero-mean Gaussian white noise. If it includes random signals, then the correct way to define the error at the end of horizon is by using an expectation as follows: $E\left\{\mathbf{e}(t+T)\right\} = 0$. However, because the random signal is assumed to be zero mean, the overall effect on $\mathbf{e}(t+T)$ is zero in the averaged sense, i.e. it is unbiased.[11] For notational simplicity, we simply write $\mathbf{e}(t+T) = 0$ without expectation. Note that T is the length of the receding-horizon interval, which is not the sampling interval in general.

There are some differences in the above formulation from the original receding-horizon problem of Ref. 6, which was not originally formulated as an estimation problem but a control problem. In the original receding-horizon formulation, the residual error is the error between a reference trajectory and an output trajectory, and the optimization variable is not a resulting model-error effect but a control input in the system. The

closed form solution of Eq. (2) is not available in general. However, by approximating the cost function, a closed form solution can be obtained.[6] Although this problem is reformulated to our model-error estimation problem, most of derivations remain the same.

At each time t, the model-error solution $\hat{\mathbf{u}}(t)$ over a finite horizon $[t,\, t+T]$ is determined on-line. Define $h \equiv T/N$ for some integer $N \geq n/m$, which is the number of sub-intervals on $[t,\, t+T]$. This lower bound guarantees the existence of the ARH solution (details can be found in Ref. 6). Define

$$L(k\,h) \equiv \mathbf{e}^T(t+k\,h)R^{-1}(t+k\,h)\mathbf{e}(t+k\,h) + \hat{\mathbf{u}}^T(t+k\,h)\,W(t+k\,h)\,\hat{\mathbf{u}}(t+k\,h) \tag{6}$$

The cost function to be minimized is approximated using a trapezoidal formula or Simpson's rule.[6]

To obtain an explicit expression for Eq. (6) in terms of the known quantities at time t, such as the current state, input, etc., we need to make the following assumptions. Since the future values of $\tilde{\mathbf{y}}(t)$ and $\mathbf{u}(t)$ are unknown in general, they are assumed to remain constant over the finite horizon $[t,\, t+T]$. Although this assumption seems to be an extremely inaccurate approximation, in the design process the length of subinterval, h, and the weights, R and/or W, are tuned appropriately for the system to be stable. The constant-over-the-interval assumption becomes less accurate as the receding-horizon step-time T increases and/or the speed of response increases. Therefore, the weights for $L(kh)$ in Eq. (6) should become larger as the index, k, increases. Our approach uses an exponential weighting scheme:

$$R_k = e^{r_p}\, R_{k-1} \tag{7a}$$

$$W_k = e^{w_p}\, W_{k-1} \tag{7b}$$

where R_0 and W_0 are assumed given, and r_p and w_p are non-negative real values, which may be time varying. For simplicity and avoiding the cross-product terms of $\hat{\mathbf{u}}(t+ih)$ and $\hat{\mathbf{u}}(t+jh)$, we assume that $G[\mathbf{x}(t+kh)] \approx G[\mathbf{x}(t)]$ and $F[\mathbf{x}(t+kh)] \approx F[\mathbf{x}(t)]$, where $F \equiv \partial\mathbf{f}/\partial\mathbf{x}$ (see Ref. 5 for details). With these assumptions, the future state can be approximated using either a repeated first-order or an rth-order Taylor series expansion, where r is the relative degree of the system.[12] After using this expansion, then the model error can be determined. Details on the expansion and the model-error solution can be found in Ref. 13.

III. Spacecraft Attitude Control

In this section the nominal control design in Ref. 9 is first summarized and then the model-error correction input using the ARH approach is derived. Next, a method is derived to choose the weighting and the length of receding-horizon interval to minimize the sensitivity function norm of the closed-loop system. Then, a stability analysis for the nonlinear system, which includes the actual dynamics, is presented. Finally, simulation results are shown to verify the new control design approach.

A. Nominal Controller Design

The spacecraft attitude kinematics and dynamics can be written as follows:[14]

$$\dot{\boldsymbol{\sigma}}(t) = \frac{1}{4}B\left[\boldsymbol{\sigma}(t)\right]\boldsymbol{\omega}(t) \tag{8a}$$

$$\dot{\boldsymbol{\omega}}(t) = -I^{-1}\left[\boldsymbol{\omega}(t)\times\right]I\boldsymbol{\omega}(t) + I^{-1}\mathbf{u}(t) + I^{-1}\hat{\mathbf{u}}(t) \tag{8b}$$

where $\boldsymbol{\sigma}(t)$ represents the Modified Rodrigues Parameter (MRP) vector, $\boldsymbol{\omega}(t)$ is the angular-velocity vector, I is the spacecraft inertia matrix, $\hat{\mathbf{u}}(t)$ is the model-error vector to be determined (which is a function of the unknown external disturbances, spacecraft moment of inertia and the angular velocity), and $\mathbf{u}(t)$ is the total control input defined by Eq. (1). The matrix $B\left[\boldsymbol{\sigma}(t)\right]$ is given by[14]

$$B\left[\boldsymbol{\sigma}(t)\right] \equiv \left[1-\sigma^2(t)\right]I_{3\times3} + 2\left[\boldsymbol{\sigma}(t)\times\right] + 2\,\boldsymbol{\sigma}(t)\boldsymbol{\sigma}^T(t) \tag{9}$$

where $I_{3\times3}$ is a 3×3 identity matrix, $\sigma^2(t) = \boldsymbol{\sigma}^T(t)\boldsymbol{\sigma}(t)$, and the inverse is given by

$$B^{-1}\left[\boldsymbol{\sigma}(t)\right] = \left[1+\sigma^2(t)\right]^{-2}\,B^T\left[\boldsymbol{\sigma}(t)\right] \tag{10}$$

For $\mathbf{a} \equiv [a_1,\, a_2,\, a_3]^T$, the cross product operator $[\mathbf{a}\times]$ is defined by

$$[\mathbf{a}\times] \equiv \begin{bmatrix} 0 & -a_3 & a_2 \\ a_3 & 0 & -a_1 \\ -a_2 & a_1 & 0 \end{bmatrix} \tag{11}$$

¿From the control design in Ref. 9, the nominal control input, which performs a feedback linearization, is given by

$$\bar{\mathbf{u}}(t) = [\boldsymbol{\omega}(t)\times]\, I\boldsymbol{\omega}(t) + I\boldsymbol{\phi}(t) \tag{12}$$

with

$$\begin{aligned} \boldsymbol{\phi}(t) = -P\boldsymbol{\omega}(t) - \left\{ \boldsymbol{\omega}(t)\,\boldsymbol{\omega}^T(t) + \left(\frac{4K}{1+\sigma^2(t)} - \frac{\omega^2(t)}{2} \right) I_{3\times 3} \right\} \boldsymbol{\sigma}(t) \\ - 4K_I B^{-1}\left[\boldsymbol{\sigma}(t)\right] \int_0^t \boldsymbol{\sigma}(\xi) d\xi \end{aligned} \tag{13}$$

where P, K, and K_I are the control gain matrices and $\omega^2(t) = \boldsymbol{\omega}^T(t)\,\boldsymbol{\omega}(t)$. After substituting this control input into the dynamics in Eq. (8), the closed-loop system becomes

$$\ddot{\boldsymbol{\sigma}}(t) = -P\dot{\boldsymbol{\sigma}}(t) - K\boldsymbol{\sigma}(t) - K_I \int_0^t \boldsymbol{\sigma}(\xi)\, d\xi + \frac{1}{4} B\left[\boldsymbol{\sigma}(t)\right]\, I^{-1}\left\{\hat{\mathbf{u}}\,(t) - \hat{\mathbf{u}}\,(t-\tau)\right\} \tag{14}$$

In Ref. 9 the inertia matrix, I, and external disturbances are estimated by an adaptive scheme, where the model parameters are updated on-line in the control law so that the closed-loop system is globally asymptotically stable. In this paper instead of using the adaptive scheme, the total model-error vector, $\hat{\mathbf{u}}(t)$, is estimated by the ARH solution and the control input is corrected using the MECS approach shown in Figure 1.

B. Model Error Determination

Setting $P = pI_{3\times 3}$, $K = kI_{3\times 3}$, and $K_I = k_I I_{3\times 3}$, where p, k, and k_I are positive constants, yields

$$\ddot{\sigma}_i(t) = -p\,\dot{\sigma}_i(t) - k\,\sigma_i(t) - k_I \int_0^t \sigma(\xi)\, d\xi + \hat{\nu}_i(t) - \hat{\nu}_i(t,\, t-\tau) \tag{15}$$

for $i = 1,\, 2,\, 3$, where

$$\hat{\boldsymbol{\nu}}(t) = \frac{1}{4} B\left[\boldsymbol{\sigma}(t)\right]\, I^{-1}\hat{\mathbf{u}}(t) \tag{16a}$$

$$\hat{\boldsymbol{\nu}}(t,\, t-\tau) = \frac{1}{4} B\left[\boldsymbol{\sigma}(t)\right]\, I^{-1}\hat{\mathbf{u}}(t-\tau) \tag{16b}$$

and $\hat{\boldsymbol{\nu}}(t) \equiv [\hat{\nu}_1(t),\, \hat{\nu}_2(t),\, \hat{\nu}_3(t)]^T$ and $\hat{\boldsymbol{\nu}}(t,\, t-\tau) \equiv [\hat{\nu}_1(t,\, t-\tau),\, \hat{\nu}_2(t,\, t-\tau),\, \hat{\nu}_3(t,\, t-\tau)]^T$. The state-space form for each axis is given by

$$\dot{\mathbf{x}}_i(t) = A_i\mathbf{x}_i(t) + B_i\,\varpi_i(t,\, t-\tau) + B_i\,\hat{\nu}_i(t) \tag{17a}$$

$$y_i(t) = C_i\,\mathbf{x}_i(t), \tag{17b}$$

for $i = 1,\, 2,\, 3$, where

$$\varpi_i(t,\, t-\tau) \equiv \breve{\nu}_i(t) - \hat{\nu}_i(t,\, t-\tau) \tag{18a}$$

$$\breve{\nu}_i(t) \equiv -k_I \int_0^t \sigma_i(\xi)\, d\xi \tag{18b}$$

$$\mathbf{x}_i(t) = \begin{bmatrix} x_{i_1}(t), & x_{i_2}(t) \end{bmatrix}^T = \begin{bmatrix} \sigma_i(t), & \dot{\sigma}_i(t) \end{bmatrix}^T \tag{18c}$$

and

$$A_i = \begin{bmatrix} 0 & 1 \\ -k & -p \end{bmatrix},\ B_i = \begin{bmatrix} 0 \\ 1 \end{bmatrix},\ C_i = \begin{bmatrix} 1 & 0 \end{bmatrix} \tag{19}$$

Usually k_I is chosen to be as small as possible so that the integral control action does not significantly affect the transient response, while also reducing the steady-state error. Therefore, in order to help simplify the analysis by keeping the order of the model equal to two, the integral control term is not used for the design process. However, it will be used in the final control law. After the vector $\hat{\boldsymbol{\nu}}(t)$ is determined, the actual model-error correction input, $\hat{\mathbf{u}}(t)$, is given by

$$\hat{\mathbf{u}}(t) = \frac{4}{\left[1 + \sigma^2(t)\right]^2} I\, B^T \left[\boldsymbol{\sigma}(t)\right] \hat{\boldsymbol{\nu}}(t) \tag{20}$$

Since the relative degree is 2, we choose the value of the subinterval N be equal to 2, and the predicted states at time $t + h$ are determined using the rth-order Taylor series expansion. Finally, the estimated model-error correction input is given by

$$\hat{\nu}_i(t) = a_1\, x_{i_1}(t) + a_2\, x_{i_2}(t) + a_3\, \varpi_i(t,\, t - \tau) + a_4\, \tilde{y}_i(t) \tag{21}$$

for $i = 1,\ 2,\ 3$, where a_1, a_2, a_3 and a_4 are functions of r_p, w_p, h and τ (given in the Appendix for the $N = 2$ case), and $\tilde{y}_i(t)$ is the i-th element of $\tilde{\mathbf{y}}(t)$. Note that Eq. (21) still retains the integral control action.

C. Design Process

Our goal is to determine r_p, w_p, h and τ that minimizes the ∞-norm of sensitivity function for the system given by Eq. (17). To accomplish this goal, the closed-loop system has to be derived. Neglecting the effects of noise on the system, then the following closed-loop transfer function is obtained:

$$y_i(t) = \frac{N_{cl}(s)}{D_{cl}(s)} \left[\hat{\nu}_i(t)\right] \equiv S(s) \left[\hat{\nu}_i(t)\right] \tag{22}$$

where $S(s)$ is sensitivity function, with

$$\begin{aligned} D_{cl}(s) &= \left[d_t(s) + a_3 n_t(s)\right] D_k(s) D_s(s) + \left[(1 - a_3)\, d_t(s) + a_3 n_t(s)\right] N_k(s) N_s(s) \\ &\quad + d_t(s)\, (a_1 + a_4 + s a_2)\, D_k(s) N_s(s) \qquad \text{(23a)} \\ N_{cl}(s) &= \left[d_t(s) + a_3 n_t(s)\right] D_k(s) D_s(s) \qquad \text{(23b)} \end{aligned}$$

The term $N_k(s)/D_k(s)$ is the transfer function of the integral control action given by Eq. (18b). Note that the nominal controller in Eq. (12) is now embedded in the system model through Eq. (17). The transfer function $N_s(s)/D_s(s)$ is equal to $C_i(sI_{2\times 2} - A_i)^{-1}B_i$. Also, $n_t(s)/d_t(s)$ is a Padé approximation of $e^{-\tau s}$ from the time delay in the MECS design. The following $(3, 3)$ Padé approximation is used:[15]

$$e^{-\tau s} \approx \frac{-\tau^3 s^3 + 12\,\tau^2 s^2 - 60\,\tau s + 120}{\tau^3 s^3 + 12\,\tau^2 s^2 + 60\,\tau s + 120} \equiv \frac{n_t(s)}{d_t(s)} \tag{24}$$

Note that all variables in Eq. (22) are evaluated at time t only now, which is due to the use of the Padé approximation for the time delay. The variables r_p, w_p, h and τ are chosen so that the ∞-norm of the sensitivity function, $||S(j\omega)||_\infty$, is minimized. For this particular problem we have found that the stable region is most affected by the values of h and r_p. Hence, we choose to hold the other variables constant.[16] Although this is strictly not an optimal approach from a parameter optimization point of view, i.e. by minimizing the sensitivity function, it allows us to visualize the effects of the most sensitive parameters in finding the required region. Further optimizations may yield better results, i.e. by performing a numerical parameter optimization to find all four parameters that minimize $||S(j\omega)||_\infty$, but our simple approach provides adequate robustness characteristics in the MECS design, which is shown through simulation. So, the parameter space for the sought values is now 2-dimensional (r_p and h). We set $k = 1.0$, $p = 3.0$ and $k_I = 0.090$, which are adopted from Ref. 9, and $w_0 = 1$, $w_p = 0.1$, $r_0 = 0.5$ and $\tau = 0.0025$ sec. The closed-loop characteristic equation is given by

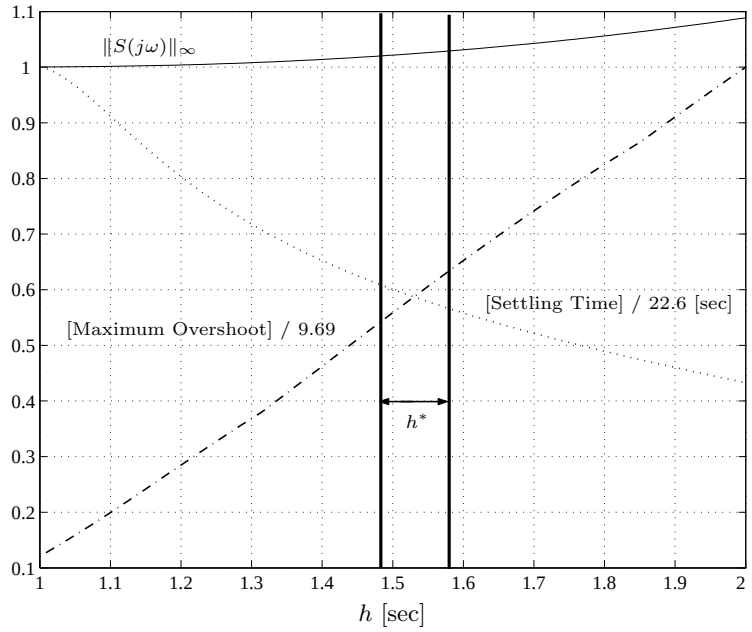

Figure 2. h vs. $\|S(j\omega)\|_\infty$, Settling Time, and Maximum Overshoot

$$
\begin{aligned}
D_{cl} = {} & \tau^3 (1 - a_3)\, s^6 + \left[\tau^3 (a_2 - 3\, a_3 + 3) + 12\, \tau^2 (1 + a_3)\right] s^5 + \left[\tau^3 (1 + a_1 - a_3 + a_4)\right. \\
& \left. + 36\, \tau^2 (36\, a_3 + 12\, a_2 + 36) + 60\, \tau (1 - a_3)\right] s^4 + \left[0.09\, \tau^3 (1 - a_3) + 12\, \tau^2 (1 + a_1 + a_3 + a_4)\right. \\
& \left. + 60\, \tau (3 + a_2 - 3\, a_3) + 120\, (1 + a3)\right] s^2 + \left[1.08\, \tau^2 (1 - a_3) + 60\, \tau (1 + a_1 - a_3 + a_4)\right. \\
& \left. + 120\ (1 + 3\, a_2 + 3\, a_3)\right] s + 10.80\, (1 - a_3)
\end{aligned} \tag{25}
$$

A stable region for Eq. (25) can now be found using linear system theory, such as the Routh-Hurwitz stability criterion, root locus, etc. After the stable region is found, by calculating $\|S(j\omega)\|_\infty$ for various values of h and r_p, we find that the norm is more sensitive to h than r_p. Figure 2 depicts h versus the normalized values of $\|S(j\omega)\|_\infty$, settling time and maximum overshoot for an impulse $\hat{\nu}(t)$ input, with r_p set to 0.1 (chosen by trial and error). To minimize the sensitivity norm the value of h has to be chosen as small as possible. However, the settling time increases as h decreases and the control input may saturate. Therefore, good values of h are in the range of $1.48 \leq h^* \leq 1.58$. By trial and error $h^* = 1.5$ sec is selected. Finally, the determined model error for $i = 1,\ 2,\ 3$ is given by

$$
\hat{\nu}_i(t) = 0.72\, x_{i_1}(t) + 2.03\, x_{i_2}(t) - 0.66\, \varpi_i(t,\, t - \tau) - 0.06\, \tilde{y}_i(t) \tag{26}
$$

It is important to note that although the design procedure to determine the gains is fairly complex, the resulting model-error correction in Eq. (26) is very simple. Also, to check the robustness with respect to various values of the time delay, τ, the roots of Eq. (25) are computed for different τ. All the poles are in the left half plane for values of τ up to 0.1 sec.

D. Nonlinear Analysis and Simulation Results

The simulations contain both modeling errors and external disturbances. The actual system is simulated using

$$
\dot{\boldsymbol{\sigma}}_a(t) = \frac{1}{4} B\left[\boldsymbol{\sigma}_a(t)\right] \boldsymbol{\omega}_a(t) \tag{27a}
$$

$$
\dot{\boldsymbol{\omega}}_a(t) = -I_a^{-1}\left[\boldsymbol{\omega}_a(t)\times\right] I_a \boldsymbol{\omega}_a(t) + I_a^{-1}\mathbf{u}(t) + I_a^{-1}\mathbf{F}(t) \tag{27b}
$$

where the subscript a denotes the actual (true) system and $\mathbf{F}(t)$ denotes an external disturbance vector. In the simulations we use the following inertia matrices taken from Ref. 9:

$$I_a = \begin{bmatrix} 30 & 10 & 5 \\ 10 & 20 & 3 \\ 5 & 3 & 15 \end{bmatrix} \text{kg-m}^2, \; I = \begin{bmatrix} 5 & 0 & 0 \\ 0 & 5 & 0 \\ 0 & 0 & 5 \end{bmatrix} \text{kg-m}^2 \tag{28}$$

where I_a and I are the true and assumed inertia matrices, respectively. The output is attitude-angle, which is simulated by $\tilde{\mathbf{y}}(t) = \boldsymbol{\sigma}_a(t) + \mathbf{w}(t)$, where $\mathbf{w}(t)$ is zero-mean Gaussian white-noise with known covariance and $\boldsymbol{\sigma}_a(t) \equiv [\sigma_{a_1}, \; \sigma_{a_2}, \; \sigma_{a_3}]^T$.

1. Stability Analysis with Nonlinear Uncertainty

The MECS scheme for the attitude control problem is developed through a linearization of the model equations. In this section an analysis of the stability of this approach is shown by incorporating the errors introduced using the actual nonlinear model in Eq. (27). To analyze the stability of the system with nonlinear uncertainty, we neglect the effects of noise on the system, so $\mathbf{w}(t) = \mathbf{0}$. Noise will be added in the simulations though to provide a more realistic scenario. For the implementation of the MECS approach in practice, the model error is determined using estimated quantities of the actual variables, which will be discussed more in the Simulation Results section. With no noise in the system and assuming that a stable estimator exists which tracks the actual output with no error, we can effectively replace the state quantities in Eq. (21) with their respective actual values. Errors arise due to the differences between the actual and assumed inertia matrices with possible external disturbances. To obtain the actual closed-loop dynamics with both inertia errors and external disturbance, the procedure outlined in Ref. 9 is followed exactly here. Using the Padé (3, 3) approximation for the time delay in the controller, the actual closed-loop dynamics for each axis due to the imperfect control from the incorrect inertia matrix are given by

$$\dot{\boldsymbol{\eta}}_i(t) = A_{\eta_i} \, \boldsymbol{\eta}_i(t) + B_{\eta_i} \, \hat{\nu}_{a_i}(t) \tag{29}$$

with

$$A_{\eta_i} \equiv \begin{bmatrix} A_{e_i} - B_{e_i} \, D_{z_i} \, \mathbf{a}^T & -B_{e_i} \, C_{z_i} \\ B_{z_i} \, \mathbf{a}^T & A_{z_i} \end{bmatrix}, \quad B_{\eta_i} \equiv \begin{bmatrix} B_{e_i} \\ 0_{3\times 1} \end{bmatrix} \tag{30a}$$

$$A_{e_i} \equiv \begin{bmatrix} 0 & 1 & 0 \\ 0 & 0 & 1 \\ -k_I & -k & -p \end{bmatrix}, \; B_{e_i} \equiv \begin{bmatrix} 0 \\ 0 \\ 1 \end{bmatrix} \tag{30b}$$

$$A_{z_i} \equiv \begin{bmatrix} 0 & 1 & 0 \\ 0 & 0 & 1 \\ -\dfrac{120 \; (1+a_3)}{(1-a_3) \; \tau^3} & -\dfrac{60}{\tau^2} & -\dfrac{12 \; (1+a_3)}{(1-a_3) \; \tau} \end{bmatrix}, \quad B_{z_i} \equiv \begin{bmatrix} 0 \\ 0 \\ 1 \end{bmatrix} \tag{30c}$$

$$C_{z_i} \equiv \left[-\frac{240 \, a_3}{(1-a_3)^2 \; \tau^3}, \quad 0, \quad -\frac{24 \, a_3}{(1-a_3)^2 \; \tau} \right], \quad D_{z_i} \equiv \frac{1}{1-a_3} \tag{30d}$$

for $i = 1, 2, 3$, where $\mathbf{a}^T \equiv [\, -a_3 \, k_I, \; a_1 + a_4, \; a_2 \,]^T$. The first three states of $\boldsymbol{\eta}_i(t)$ correspond to the quantities given by $\left[\int_0^t \sigma_{a_i}(\xi) d\xi, \; \sigma_{a_i}(t), \; \dot{\sigma}_{a_i}(t) \right]^T$ and the last three states correspond to states from the Padé (3, 3) approximation in Eq. (24). Note that the model-error correction of Eq. (21) is embedded in A_{z_i}, B_{z_i}, C_{z_i} and D_{z_i}. The quantity $\hat{\nu}_{a_i}(t)$ is the i-th element of

$$\hat{\boldsymbol{\nu}}_a(t) \equiv \frac{1}{4} B \left[\boldsymbol{\sigma}_a(t) \right] I^{-1} \hat{\mathbf{u}}_a(t) \tag{31}$$

where $\hat{\mathbf{u}}_a(t)$ is the actual model error, computed by comparing Eqs. (8b) and (27b):

$$\begin{aligned} \hat{\mathbf{u}}_a(t) = & - \left[\boldsymbol{\omega}_a(t) \times \right] \delta I_1 \, \boldsymbol{\omega}_a(t) - I \, \delta I_2 \left[\boldsymbol{\omega}_a(t) \times \right] I \boldsymbol{\omega}_a(t) - I \, \delta I_2 \left[\boldsymbol{\omega}_a(t) \times \right] \delta I_1 \, \boldsymbol{\omega}_a(t) \\ & + I \, \delta I_2 \, \mathbf{u}(t) + (I_{3\times 3} + I \, \delta I_2) \, \mathbf{F}(t) \end{aligned} \tag{32}$$

where δI_1 and δI_2 are inertia errors, defined by

$$\delta I_1 \equiv I_a - I \tag{33a}$$

$$\delta I_2 \equiv I_a^{-1} - I^{-1} \tag{33b}$$

By these definitions $\delta I_2 = -\left(I_{3\times3} + \delta I_1^{-1}\, I\right)^{-1}\, I^{-1}$. Using Eq. (32) in Eq. (16a) drives the assumed model states to the actual states, as expected.

It is important to note that Eq. (29) represents the actual dynamics of Eq. (27) using the nominal controllers of Eqs. (12) and (21), combined with the actual model errors. Equation (29) is a bit deceiving since $A_{\eta_i}\,\boldsymbol{\eta}_i(t)$ is a linear term. This term arises from the fact that Eq. (13) is formulated such that the closed-loop system has some desired linear characteristics when no model errors and/or external disturbances are present in the system.[9] However, all the nonlinear terms still exist through $\hat{\nu}_{a_i}(\mathrm{t})$. If no modeling or disturbances errors exist, then the first three states of Eq. (29) yield the desired closed-loop dynamics $\ddot{\sigma}_{a_i}(t) + p\,\dot{\sigma}_{a_i}(t) + k\,\sigma_{a_i}(t) + k_I\,\int_0^t \sigma_{a_i}(\xi)d\xi = 0$ for each axis, analogous to the approach shown in Ref. 9. To provide a stability proof for Eq. (29), the subsequent definitions and theorems are summarized, where the proof of each of the following can be found in Ref. 17.

Quadratically Stable; Consider the following system with nonlinear uncertainty $\Delta\mathbf{f}[\boldsymbol{\eta}(t)]$:

$$\dot{\boldsymbol{\eta}}(t) = A_\eta\,\boldsymbol{\eta}(t) + \Delta\mathbf{f}[\boldsymbol{\eta}(t)] \tag{34}$$

where A_η is the block diagonal matrix composed by A_{η_i}, for $i = 1, 2, 3$, and $\Delta\mathbf{f}[\boldsymbol{\eta}(t)] \equiv E_f\,\boldsymbol{\delta}\,[\boldsymbol{\eta}(t)]$ is a C^0 function, $\boldsymbol{\eta}(t) \equiv [\boldsymbol{\eta}_1^T(t),\, \boldsymbol{\eta}_2^T(t),\, \boldsymbol{\eta}_3^T(t)]^T$, and $\boldsymbol{\delta}\,[\boldsymbol{\eta}(t)]$ is a element of the following set:

$$\Omega \equiv \{\, \boldsymbol{\delta}\,[\boldsymbol{\eta}(t)] \mid \|\boldsymbol{\delta}\,[\boldsymbol{\eta}(t)]\,\|_\infty \leq \|N_f\,\boldsymbol{\eta}(t)\|_\infty,\ \forall\ \boldsymbol{\eta}(t)\} \tag{35}$$

where N_f is a constant matrix. For our particular system in Eq. (29) we have $\Delta\mathbf{f}[\boldsymbol{\eta}(t)] \equiv B_\eta\,\hat{\boldsymbol{\nu}}_a(t)$, where B_η is the block diagonal matrix composed of B_{η_i}, for $i = 1, 2, 3$, and $\hat{\boldsymbol{\nu}}_a(t)$ is given by Eq. (31). Hence, E_f is equal to B_η. Note that nonlinearities exist in the particular $\Delta\mathbf{f}[\boldsymbol{\eta}(t)]$ from the definition in Eq. (32). The system, Eq. (34), is said to be quadratically stable if there exists a positive-definite symmetric matrix $P_q > 0$ such that

$$\{A_\eta\,\boldsymbol{\eta}(t) + \Delta\mathbf{f}[\boldsymbol{\eta}(t)]\}^T\ P_q\,\boldsymbol{\eta}(t) + \boldsymbol{\eta}^T(t)\,P_q\ \{A_\eta\,\boldsymbol{\eta}(t) + \Delta\mathbf{f}[\boldsymbol{\eta}(t)]\} < 0 \tag{36}$$

for all nonzero $\boldsymbol{\eta}(t) \in \Re^{3n}$ and all admissible nonlinear uncertainty $\Delta\mathbf{f}[\boldsymbol{\eta}(t)]$.

Quadratic Cost Matrix, P_q; A positive definite matrix $P_q > 0$ is said to be a quadratic cost matrix for Eq. (34) and the following cost function:

$$J_q = \int_0^\infty \boldsymbol{\eta}^T(t)\,Q_q\,\boldsymbol{\eta}(t)\,dt \tag{37}$$

where $Q_q \geq 0$, if

$$\{A_\eta\,\boldsymbol{\eta}(t) + \Delta\mathbf{f}[\boldsymbol{\eta}(t)]\}^T\ P_q\,\boldsymbol{\eta}(t) + \boldsymbol{\eta}^T(t)\,P_q\ \{A_\eta\,\boldsymbol{\eta}(t) + \Delta\mathbf{f}[\boldsymbol{\eta}(t)]\} < -\boldsymbol{\eta}^T(t)\,Q_q\,\boldsymbol{\eta}(t) \tag{38}$$

for all nonzero $\boldsymbol{\eta}(t) \in \Re^{3n}$ and all admissible nonlinear uncertainty $\Delta\mathbf{f}[\boldsymbol{\eta}(t)]$. Checking all possible inertia errors and control gains for all admissible nonlinear uncertainty is an intractable problem to solve. Thus, only the specific inertias given by Eq. (28) and assumed control gains are checked. For our particular controller gains, A_{η_i} is given by

$$A_{\eta_i} = \begin{bmatrix} 0 & 1 & 0 & 0 & 0 & 0 \\ 0 & 0 & 1 & 0 & 0 & 0 \\ -0.13 & -1.40 & -4.23 & -70447.0 & 0 & -9234.0 \\ 0 & 0 & 0 & 0 & 512.0 & 0 \\ 0 & 0 & 0 & 0 & 0 & 4096.0 \\ 0.015 & 0.17 & 0.51 & -715.4 & -2344 & -937.7 \end{bmatrix} \tag{39}$$

The Cost Function Bound; If $P_q > 0$ is a quadratic cost matrix for the nonlinear uncertain system, Eq. (34), then the system is quadratically stable and the cost function is bounded by

$$J_q \leq \boldsymbol{\eta}^T(0)\, P_q\, \boldsymbol{\eta}(0) \tag{40}$$

and if the system is quadratically stable, then there exists a quadratic cost matrix.

H_∞ *Norm Bound Condition*; For the system, Eq. (34), there exists a quadratic cost matrix, $P_q > 0$, if and only if the following conditions hold: 1) A_η is a stable matrix, and 2) the following H_∞ norm bound is satisfied for some $\epsilon > 0$

$$\left\| \begin{bmatrix} N_f \\ \sqrt{\epsilon}\, Q_q \end{bmatrix} (s\, I_{n\times n} - A_\eta)^{-1}\, E_f \right\|_\infty < 1 \tag{41}$$

Then, for such ϵ, the Riccati equation

$$A_\eta^T\, P_q + P_q\, A_\eta + \epsilon\, P_q\, E_f\, E_f^T\, P_q + \frac{1}{\epsilon}\, N_f^T\, N_f = -Q_q \tag{42}$$

has a solution.

The particular matrix A_η, formed from the sub-matrices in Eq. (39), is stable. So, the first stability condition is satisfied. For the cost function, J_q, the first three states for each axis are penalized, which are the integral, the proportional and the derivative of the MRP parts for each axis. Then Q_q is given by the block diagonal matrix composed by Q_{q_i}, which is as follows:

$$Q_{q_i} = \begin{bmatrix} I_{3\times 3} & 0_{3\times 3} \\ 0_{3\times 3} & 0_{3\times 3} \end{bmatrix} \tag{43}$$

There is no systematic way to determine the quantities N_f and ϵ, described in the previously mentioned definitions and theorems. In fact there are many possible solutions for our particular system. One of the obviously best ways is to find the largest possible admissible bound of the nonlinear uncertainty by formulating the problem as an maximization problem, such that N_f and ϵ maximize $\|N_f\, \boldsymbol{\eta}(t)\|_\infty$, subject to the existence of P_q that satisfies Eq. (42). However, solving this maximization problem is difficult, so instead we use the following heuristic method. First, fix ϵ equal to some constant, which we choose to be 0.001, and then find N_f such that the following condition holds for all time:

$$\Delta\nu_i(t) \equiv \text{sgn}\left\{\|N_f\, \boldsymbol{\eta}(t)\|_\infty - \|\hat{\nu}_{a_i}(t)\|_\infty\right\} = 1 \tag{44}$$

or at least holds for as long as possible, which is checked by nonlinear simulation. Equation (44) is merely used to maximize $\|N_f\, \boldsymbol{\eta}(t)\|_\infty$ in a heuristic sense. But even if Eq. (44) is satisfied for all time (or a fraction of the time) using a trial N_f, the matrix P_q must still be shown to exist by satisfying Eq. (42).

Clearly, if $\mathbf{F}(t)$ is not a function of the states, the norm bounded uncertainty assumption in Eq. (44) is not satisfied with this type of external disturbance. This does not mean that the system is unstable though, which will be shown through simulation. For other disturbances that are a function of the states, e.g. aerodynamic drag, it may be possible to analytically prove stability. The norm bound can be checked on a case-by-case basis, which depends on the particular aspects of the disturbances present in the actual system. For our particular inertia matrices and assumed control gains, without the external disturbance or sensor noise, after various numerical trials the following N_f is obtained:

$$N_f = \text{diag}\left[N_{f_1},\ N_{f_2},\ N_{f_3}\right] \tag{45}$$

where

$$N_{f_i} = \begin{bmatrix} \text{diag}\,[0.248,\ 2.250,\ 8.160] & 0_{3\times 3} \end{bmatrix} \tag{46}$$

and diag denotes the diagonal matrix. The time histories of each $\Delta\nu_i(t)$ is shown in Figure 3. For this case, when $t > 6.3$ sec, the nonlinear uncertainties are inside the norm bound. The minus sign of $\Delta\nu_i(t)$ at the beginning is due to the large uncertainty in the inertia matrix. The norm bound condition, Eq. (41), with the given matrices is still satisfied though, since the computed ∞-norm is 0.9982. Moreover, the cost function, which is given by Eq. (37), is bounded by Eq. (40). To obtain P_q in Eqs. (40) and (42), the Special

Algebraic Riccati Equation, Eq. (42), is solved. The solution for P_q gives a symmetric and positive definite matrix (the smallest eigenvalue is 29.20). Therefore, the quadratic cost function, Eq. (37), is bounded by

$$J_q \leq 2.746 \times 10^4 \left\|\boldsymbol{\sigma}_a(0)\right\|_2^2 + 5.815 \times 10^3 \, \boldsymbol{\sigma}_a^T(0) \, \dot{\boldsymbol{\sigma}}_a(0) + 5.739 \times 10^3 \left\|\dot{\boldsymbol{\sigma}}_a(0)\right\|_2^2 \tag{47}$$

Hence, for the norm bounded uncertainty by the second condition for quadratic stability, the closed-loop system is stable.

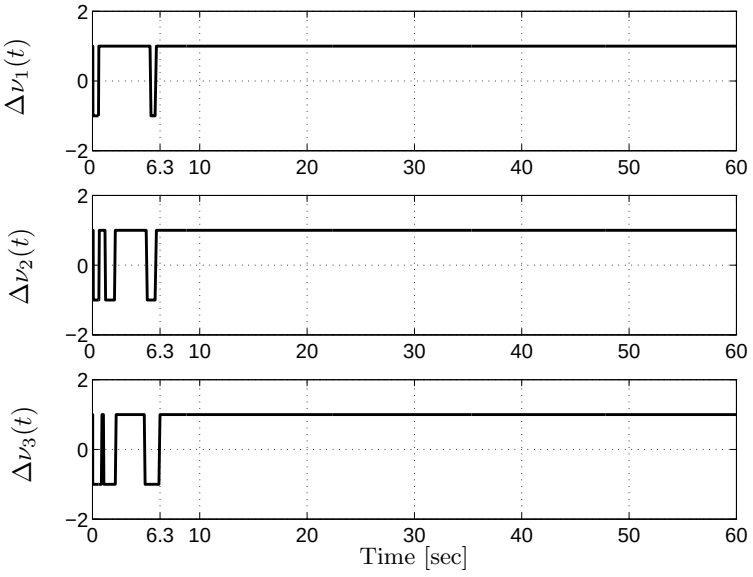

Figure 3. Time History of $\Delta\nu_i(t)$

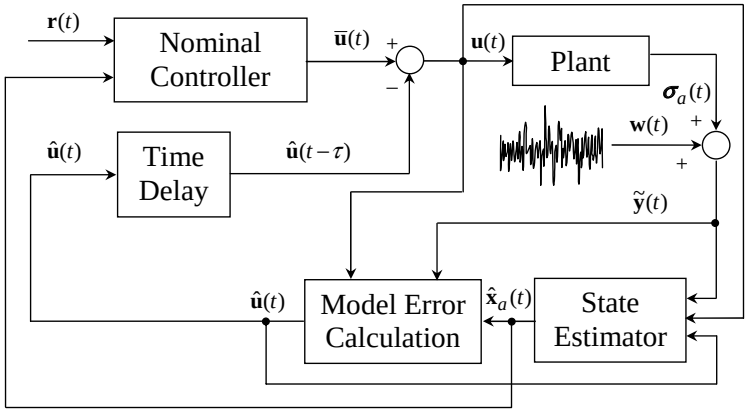

Figure 4. MECS Block Diagram with State Estimator

2. Simulation Results

In this section simulation results are shown. In order to provide a more realistic simulation, a state estimator is used to provide full-state information, which is required in the control scheme. A block diagram of this approach is given in Figure 4, where $\hat{\mathbf{x}}_a(t)$ denotes the estimate of $\mathbf{x}_a(t) \equiv [\boldsymbol{\sigma}_a^T(t), \, \boldsymbol{\omega}_a^T(t)]^T$. A Kalman filter using the dynamics model is designed for state estimation, which includes a filtered attitude and estimated angular velocity (details on tuning the filter gains are beyond the scope of this paper). The state estimate is now used in the determined model error of Eqs. (20) and (26) and in the nominal controller of Eq. (12). For the simulations we set $\mathbf{r}(t) = \mathbf{0}$. The initial MRP is $\boldsymbol{\sigma}_a(0) = [-0.3, \, -0.4, \, 0.2\,]^T$ and the initial angular

velocity is $\boldsymbol{\omega}_a(0) = [0.2,\, 0.2,\, 0.2]^T$ rad/sec. A constant external disturbance of $\mathbf{F}(t) = [2,\, 1,\, -1]^T$ N·m has been used (consistent with Ref. 9). For the simulation the noise variance for the MRP measurement is given by 1.23×10^{-5}.[18] The state estimation errors and 3σ bounds are shown in Figure 5. Without using an angular-velocity sensor, such as a three-axis gyro, the rate estimation error bound is about $\pm 1.2^\circ$/sec. If this error is too large, then gyro measurements should be employed.

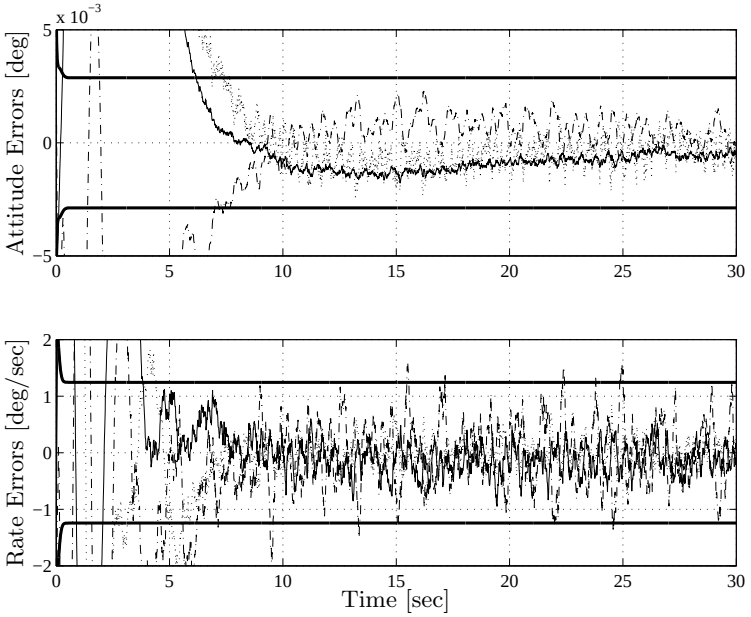

Figure 5. Estimation Errors and 3σ Bounds

The model-error components at the initial time are all set to zero. The control histories for each case are shown in Figure 6(a). The NO ERRORS case corresponds to using the nominal control design only with no inertia errors or external disturbances, but with measurement noise included. The MECS OFF case corresponds to using the nominal controller only with both inertia errors and external disturbances. The MECS ON case corresponds to using the nominal controller and the model-error correction part with the same situation as the MECS OFF case. The NO ERRORS case has more transient behaviors in the control histories than the other cases, but the response trajectories of the MRPs are nearly identical for the MECS ON and NO ERRORS cases, as shown in Figure 6(b). With MECS OFF far larger transients are present in the trajectories of the MRPs. The MRP norm histories for each case are shown in Figure 6(c). When no errors are present we expect that the steady-state errors decay to values near the noise levels of the output, due to the integral control action. However, because of modeling errors, the steady-state values have much larger errors. In contrast the steady-state values for the MECS ON case are about 85% smaller than the MECS OFF case, and the settling time of the MECS ON case is slightly faster than the MECS OFF case. Clearly, the MECS ON case provides the best performance when modeling errors and disturbances are present. Note that in Ref. 9 the MRP error with the adaptive control keeps decreasing below the MECS ON case shown in this paper. The main reason for this is that perfect state information with no measurement noise is used in Ref. 9. But, this is not the case in the simulations, which provide a more realistic scenario of an actual spacecraft application.

As an additional test, instead of a constant disturbance, we employ a time-varying external disturbance, given by

$$\mathbf{F}(t) = \begin{bmatrix} 2 + \frac{1}{5}\sin\left(\frac{t}{7}\right) \\ 1 + \frac{1}{10}\sin\left(\frac{t}{7} + \frac{\pi}{4}\right) \\ -1 - \frac{1}{10}\cos\left(\frac{t}{7}\right) \end{bmatrix} \quad \text{N·m} \tag{48}$$

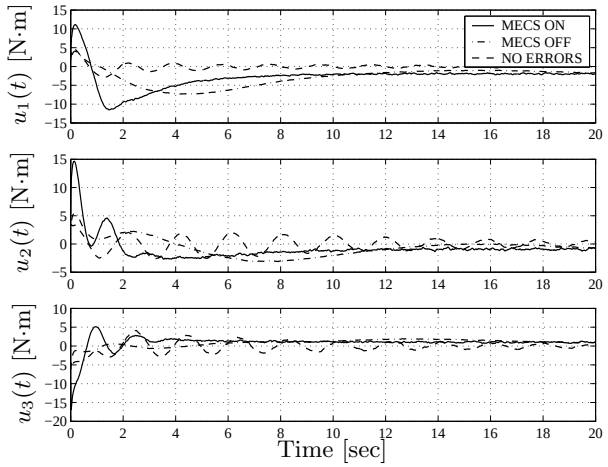

(a) Control Input Time History

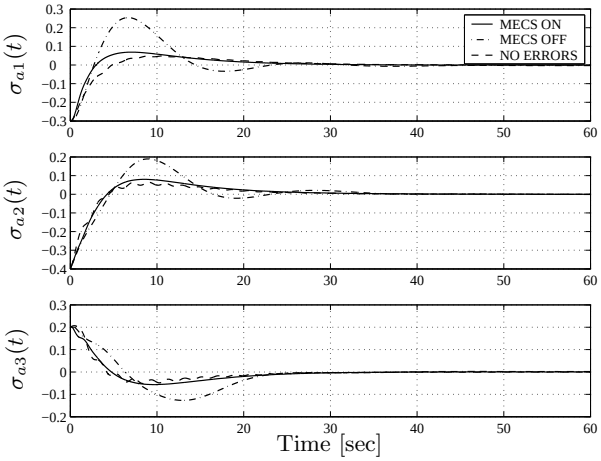

(b) MRP Time History

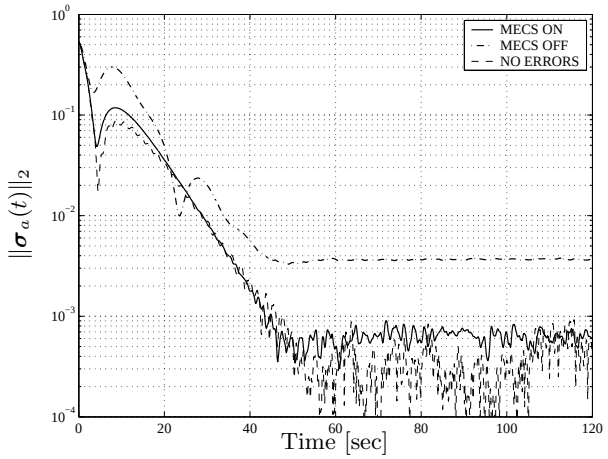

(c) MRP Norm with Constant Disturbance

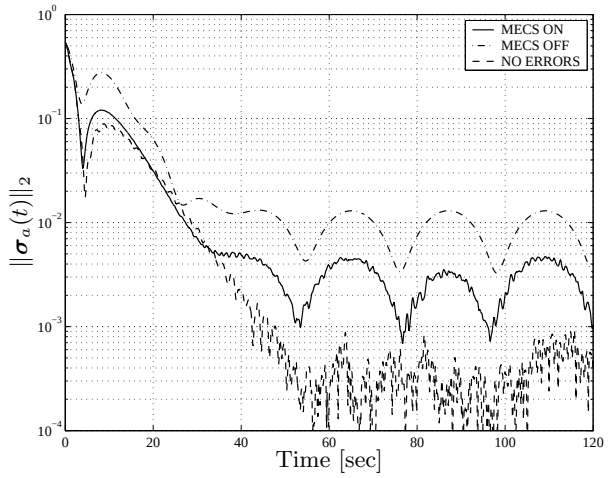

(d) MRP Norm with Time Varying Disturbance

Figure 6. Responses with Inertia Errors and Various Disturbance

The above external disturbance has the constant parts of the external disturbance scenario in Ref. 9 with the additional 10% amplitude sinusoidal parts. The frequency is chosen such that the magnitude of the output is maximized, i.e. worst case frequency. All of the other conditions remain the same as before, including all control and filter gains, i.e. no modifications have been made to the controllers used in the previous simulation. The real power of the MECS approach is that it can compensate for time-varying disturbances, unlike the parameter adaptive approach shown in Ref. 9. The MRP norm histories for this simulation are shown in Figure 6(d). The error fluctuates because of the time-varying components in the external disturbance. Still, the MECS ON case clearly outperforms the MECS OFF case.

The stability of the actual closed-loop system in Eq. (29) is now shown by evaluating the left side of Eq. (36) using the incorrect inertia matrix as well as the disturbance inputs. The top plot of Figure (7) shows this quantity with the constant disturbance added, while the bottom plot shows this quantity using the time varying disturbance. Clearly, the inequality is satisfied using the inertia errors with either type of disturbance added. Note that in order to fully prove stability, Eq. (36) must be satisfied for all admissible nonlinear uncertainty. Still, satisfying this inequality signifies confidence that asymptotic stability can be provided for a class of disturbance inputs.

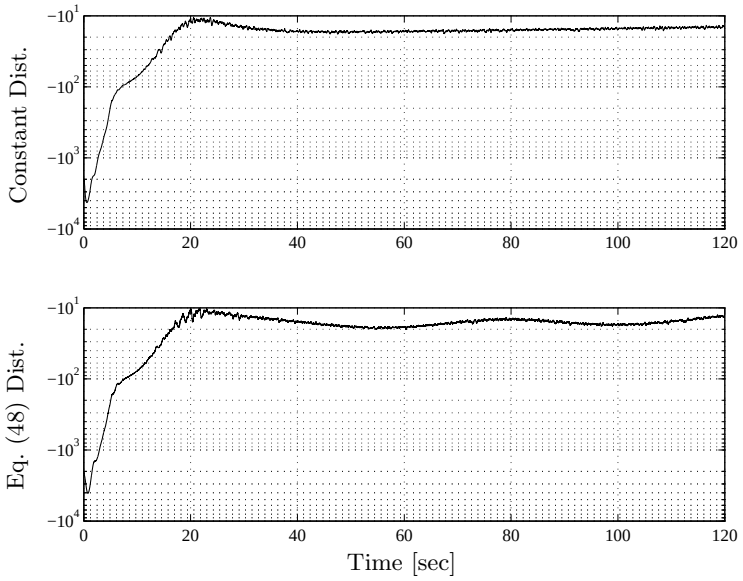

Figure 7. Plots of the Left Side of Eq. (36) for Various Disturbances

IV. Conclusions

A new approach for the robust attitude control of a maneuvering spacecraft was shown. The approach was based upon a technique known as model-error control synthesis, which corrects the nominal control input to mitigate the effects of modeling errors and disturbances. The main advantage of this approach for the attitude control problem, over existing adaptive methods, is its ability to handle both inertia modeling errors and time-varying disturbances. Although the design of the gains is fairly complicated, the resulting model-error correction law for this problem is simple. Realistic simulation results, involving angle-only type observations with noise, indicated that a nominal controller combined with the model-error control synthesis approach produced robust transient response behaviors, and the steady-state attitude errors were much smaller than the nominal controller only case.

Acknowledgements

This work was supported by a National Science Foundation (NSF) grant (Award #0201361) through the Civil and Mechanical Systems Division. The authors greatly appreciate this support. Also, the authors wish to thank Panagiotis Tsiotras from Georgia Tech for many helpful comments and suggestions.

References

[1]Crassidis, J. L., "Robust Control of Nonlinear Systems Using Model-Error Control Synthesis," *Journal of Guidance, Control, and Dynamics*, Vol. 22, No. 4, 1999, July-Aug., pp. 595–601.

[2]Crassidis, J. L. and Markley, F. L., "Predictive Filtering for Nonlinear Systems," *Journal of Guidance, Control, and Dynamics*, Vol. 20, No. 3, May-June 1997, pp. 566–572.

[3]Crassidis, J. L., Markley, F. L., Anthony, T. C., and Andrews, S. F., "Nonlinear Predictive Control of Spacecraft," *Journal of Guidance, Control, and Dynamics*, Vol. 20, No. 6, May-June 1997, pp. 1096–1103.

[4]Kim, J. and Crassidis, J. L., "Linear Stability Analysis of Model-Error Control Synthesis," *AIAA Guidance, Navigation and Contol Conference*, Denver, CO, Aug. 2000, AIAA-2000-3963.

[5]Kim, J. and Crassidis, J. L., "Model-Error Control Synthesis Using Approximate Receding-Horizon Control Laws," *AIAA Guidance, Navigation and Contol Conference*, Montreal, QB, Canada, Aug. 2001, AIAA-2001-4220.

[6]Lu, P., "Approximate Nonlinear Receding-Horizon Control Laws in Closed Form," *International Journal of Control*, Vol. 71, No. 1, 1998, pp. 19–34.

[7]Wie, B., *Space Vehicle Dynamics and Control*, chap. 7, American Institute of Aeronautics and Astronautics, Inc., New

York, NY, 1998.

[8]Ahmed, J., Coppola, V. T., and Bernstein, D. S., "Adaptive Asymptotic Tracking of Spacecraft Attitude Motion with Inertia Matrix Identification," *Journal of Guidance, Control, and Dynamics*, Vol. 21, No. 5, Sept.-Oct. 1998, pp. 684–961.

[9]Schaub, H., Akella, M. R., and Junkins, J. L., "Adaptive Control of Nonlinear Attitude Motions Realizing Linear Closed Loop Dynamics," *Journal of Guidance, Control, and Dynamics*, Vol. 24, No. 1, Jan.-Feb. 2001, pp. 95–100.

[10]Kim, J., Kim, J., and Crassidis, J. L., "Disturbance Accommodating Sliding Mode Controller for Spacecraft Attitude Maneuvers," *Proceedings of the AAS/GSFC 13th International Symposium on Space Flight Dynamics*, NASA, May 1998, CP1998-206858, pp. 119–131.

[11]Crassidis, J. L. and Junkins, J. L., *Optimal Estimation of Dynamic Systems*, chap. 2, Chapman & Hall/CRC, Boca Raton, FL, 2004, pp. 74–75.

[12]Isidori, A., *Nonlinear Control System*, chap. 5, Springer-Verlag, Berlin, 3rd ed., 1990, pp. 220–221.

[13]Kim, J. and Crassidis, J. L., "Robust Spacecraft Attitude Control Using Model-Error Control Synthesis," *AIAA Guidance, Navigation and Contol Conference*, Monterey, CA, Aug. 2002, AIAA-2002-4576.

[14]Schaub, H. and Junkins, J. L., "Stereographic Orientation Parameters for Attitude Dynamics: A Generalization of the Rodrigues Parameters," *Journal of the Astronautical Sciences*, Vol. 44, No. 1, Jan.-March 1996, pp. 1–19.

[15]Wang, Z. and Hu, H., "Robust Stability Test for Dynamic Systems with Short Delay by Using Padé Approximation," *Nonlinear Dynamics*, Vol. 18, No. 6, 1999, pp. 275–287.

[16]Kim, J. and Crassidis, J. L., "Fundamental Relation of Approximate Receding Horizon Optimization to The Simple Mass Spring Damper System," *AIAA Guidance, Navigation and Contol Conference*, Austin, TX, Aug. 2003, AIAA-2003-5663.

[17]Xue, A., Lin, Y., and Sun, Y., "Quadratic Guaranteed Cost Analysis for a Class of Nonlinear Uncertain Systems," *Proceeings of the 2001 IEEE International Conference on Control Applications*, IEEE, Mexico City, Mexico, September 2001.

[18]Crassidis, J. L. and Markley, F. L., "Predictive Filtering for Attitude Estimation Without Rate Sensors," *Journal of Guidance, Control, and Dynamics*, Vol. 20, No. 3, Nov.-Dec. 1997, pp. 522–527.

Appendix

$$
\begin{aligned}
a_1 = \big[& k\,\left(r_0\,w_0\,e^{r_p+w_p}\,k^2+1\right)\,h^6 + 4\,r_0\,w_0\,e^{r_p+w_p}\,p\,k^2\,h^5 - 2\,\left(7\,r_0\,w_0\,e^{r_p+w_p}\,k^2\right. \\
& \left.-2\,r_0\,w_0\,e^{r_p+w_p}\,p^2\,k+1\right)\,h^4 - 28\,r_0\,w_0\,e^{r_p+w_p}\,p\,k\,h^3 + 52\,r_0\,w_0\,e^{r_p+w_p}\,k\,h^2 \\
& + 8\,r_0\,w_0\,e^{r_p+w_p}\,p\,h - 24 r_0\,w_0\,e^{r_p+w_p}\big]\,/d_a
\end{aligned} \tag{49a}
$$

$$
\begin{aligned}
a_2 = \big[& p\,\left(r_0\,w_0\,e^{r_p+w_p}\,k^2+1\right)\,h^6 + 2\,\left(2\,r_0\,w_0\,e^{r_p+w_p}\,p^2\,k - r_0\,w_0\,e^{r_p+w_p}\,k^2 - 1\right)\,h^5 \\
& + 2\,\left(2\,r_0\,w_0\,e^{r_p+w_p}\,p^3 - 9\,r_0\,w_0\,e^{r_p+w_p}\,p\,k\right)\,h^4 + 4\,\left(5\,r_0\,w_0\,e^{r_p+w_p}\,k\right. \\
& \left.-7\,r_0\,w_0\,e^{r_p+w_p}\,p^2\right)\,h^3 + 64\,r_0\,w_0\,e^{r_p+w_p}\,p\,h^2 - 48\,r_0\,w_0\,e^{r_p+w_p}\,h\big]\,/d_a
\end{aligned} \tag{49b}
$$

$$
\begin{aligned}
a_3 = \big[& -\left(r_0\,w_0\,e^{r_p+w_p}\,k^2+1\right)\,h^6 - 4\,r_0\,w_0\,e^{r_p+w_p}\,p\,k\,h^5 + 2\,\left(7\,r_0\,w_0\,e^{r_p+w_p}\,k\right. \\
& \left.-2\,r_0\,w_0\,e^{r_p+w_p}\,p^2\right)\,h^4 + 28\,r_0\,w_0\,e^{r_p+w_p}\,p\,h^3 - 48\,r_0\,w_0\,e^{r_p+w_p}\,h^2\big]\,/d_a
\end{aligned} \tag{49c}
$$

$$
a_4 = 2\,\left[h^4 - 2\,r_0\,w_0\,e^{r_p+w_p}\,k\,h^2 - 4\,r_0\,w_0\,e^{r_p+w_p}\,p\,h + 12\,r_0\,w_0\,e^{r_p+w_p}\right]\,/d_a \tag{49d}
$$

where

$$
\begin{aligned}
d_a = & \left(r_0\,w_0\,e^{r_p+w_p}\,k^2+1\right)\,h^6 + 4\,r_0\,w_0\,e^{r_p+w_p}\,p\,k\,h^5 + 4\,r_0\,w_0\,e^{r_p+w_p}\,\left(p^2-3\,k\right)\,h^4 \\
& - 24\,r_0\,w_0\,e^{r_p+w_p}\,p\,h^3 + 2\,r_0\,w_0\,e^{r_p}\,\left(18\,e^{w_p}+e^{r_p}\right)\,h^2
\end{aligned} \tag{50}
$$